Scaling up the Banded Matrix Factorization Mechanism for Differentially Private ML

Ryan McKenna*

Abstract

DP-BANDMF offers a powerful approach to differentially private machine learning, balancing privacy amplification with noise correlation for optimal noise reduction. However, its scalability has been limited to settings where the number of training iterations is less than 10^4 . In this work, we present techniques that significantly extend DP-BANDMF's reach, enabling use in settings with and over 10^6 training iterations. Our enhanced implementation, coupled with extensive experiments, provides clear guidelines on selecting the optimal number of bands. These insights offer practitioners a deeper understanding of DP-BANDMF's performance and how to maximize its utility for privacy-preserving machine learning.

1 Introduction

Differential privacy (DP) is essential for protecting sensitive data in machine learning. The Banded Matrix Factorization mechanism (DP-BANDMF) [5] offers a compelling DP solution, outperforming both DP-SGD [1] and DENSE-DP-MF [8, 6] by strategically balancing privacy amplification with noise correlation. However, DP-BANDMF's scalability has hindered its wider use. Existing DP-BANDMF implementations face computational bottlenecks stemming from an expensive optimization problem linked to the $n \times n$ strategy matrix C (where n is the number of training iterations), requiring $O(n^3)$ time and $O(n^2)$ memory to evaluate the expected error, limiting its use to approximately 10^4 training iterations. Additionally, during training, DP-BANDMF incurs an $O(b \cdot d)$ memory overhead (where b is the number of bands in C, and d is model dimensionality), which is $b \times$ more than DP-SGD but $n/b \times$ less than DENSE-DP-MF. In this work, we develop techniques to enhance DP-BANDMF's scalability:

- Efficient Optimization: We exploit efficient inverse-matrix-vector products with banded matrices to reduce the per-iteration complexity of strategy optimization to $O(n^2 \cdot b)$ time and $O(n \cdot b)$ space. This innovation allows scaling DP-BANDMF to approximately 10^5 training iterations. Our method extends to any parameterized matrix class supporting such efficient computations.
- Toeplitz Approximation: For scenarios demanding even more iterations (up to and beyond 10^6), we trade off some accuracy for extreme scalability using Banded Toeplitz matrices. Their structure enables $O(n \cdot b)$ time and O(n) space complexity during strategy optimization. Experiments show the approximation quality loss to be less than 4% in terms of expected error.
- **Distributed Noise Generation**: Prior implementations of DP-MF-style mechanisms add noise on a single machine, even when training is coordinated across 1000's of machines [9, 6]. We show how to effectively distribute the noise generation process, allowing DP-BANDMF to effectively take advantage of multi-machine environments common in large scale training regimes, and scale to larger models and more bands than was previously possible.
- **Practical Guidance**: We conduct comprehensive experiments on expected error, and use these results to provide a more complete picture of the performance characteristics of DP-BANDMF

^{*}Google Research, mckennar@google.com

Algorithm 1 Banded Inverse Multiplication [5]

```
Input: b-Banded matrix \mathbf{C} \in \mathbb{R}^{n \times n}, stream of vectors \mathbf{z}_1, \dots, \mathbf{z}_n \in \mathbb{R}^d, where \mathbf{Z} is the matrix with rows \mathbf{z}_i.

Output: \mathbf{Y} = \mathbf{C}^{-1}\mathbf{Z}, one row at a time.

for i = 1, \dots, n do

\mathbf{y}_i = (\mathbf{z}_i - \sum_{j=i-b+1}^{i-1} C_{ij}\mathbf{y}_j)/C_{ii}

yield \mathbf{y}_i
```

Figure 1: Algorithm for streaming inverse matrix multiplication by a banded matrix. To simplify the presentation, we use the convention that out-of-bounds indexing into a matrix or vector returns 0.

than prior work on MF-style mechanisms, which have primarily focused on the few-epoch regime. We demonstrate that optimal b values often fall within practical memory constraints, making DP-BANDMF's overhead manageable for real-world use.

2 Background

We assume the reader has familiarity with differential privacy [12, 13]. DP-SGD, DENSE-DP-MF and DP-BANDMF will be summarized below.

2.1 Training Dynamics

Both DP-SGD and DENSE-DP-MF are differentially private variants of the popular SGD algorithm.

DP-SGD adds i.i.d. Gaussian noise to the (clipped + aggregated) minibatch gradients² during training to protect privacy. To relate DP-SGD to DENSE-DP-MF and DP-BANDMF, it is useful think about this process in terms of the $n \times d$ matrix \mathbf{Z} of i.i.d. Gaussian samples, where n is the number of training iterations and d is the model dimensionality. In iteration i of DP-SGD, we add the i^{th} row of \mathbf{Z} to our current minibatch gradient. The magnitude of the Gaussian noise is determined by the clipping parameter (assumed WLOG to be 1) and the function σ_{SGD} , defined below:

Definition 2.1 (Poisson Sampled DP-SGD). Let k be the target number of rounds each user/example participates, and n be the number of training iterations. Then in each round of training, a minibatch of users/examples is sampled with probability k/n. We define $\sigma_{SGD}(\epsilon, \delta, k, n)$ to be the noise multiplier required for DP-SGD to achieve the target privacy guarantee under these assumptions.

In practice σ_{SGD} is computed using numerical privacy accounting methods such as the PLD accountant [38, 11] or the RDP accountant [34]. The ratio σ_{SGD}/k is a measure of the signal-to-noise ratio. In general, this quantity monotonically decreases with k, but for sufficiently large $k \gtrsim \sqrt{n\epsilon}$ it is roughly flat [36, Figure 1] thanks to privacy amplification by sampling. The main limitation of DP-SGD is that its utility rapidly degrades when training with small batch sizes where $k < \sqrt{n\epsilon}$.

DENSE-DP-MF and DP-BANDMF are alternatives to DP-SGD that work more favorably in the small-batch regime. These mechanisms are characterized by a *strategy matrix* \mathbf{C} (usually $n \times n$ and lower triangular), and the training dynamics are the same as DP-SGD, except we use $\mathbf{C}^{-1}\mathbf{Z}$ in place of \mathbf{Z} . The noise added by these mechanisms is thus *correlated across iterations*.

While it was useful to describe DP-SGD in terms of the matrix \mathbf{Z} , in practice \mathbf{Z} is never materialized explicitly, but rather one row at a time during training. In contrast, DENSE-DP-MF may require materializing both \mathbf{Z} and $\mathbf{C}^{-1}\mathbf{Z}$ explicitly ³, which can be prohibitively expensive for large models and many training iterations. The training-time space complexity of DP-BANDMF is somewhere in

²One notable difference between Poisson Sampled DP-SGD and non-private training is the presence of variable batch sizes, which can be tricky to incorporate into modern ML infrastructure.

³this can be avoided when using pseudo random-number-generators with known seeds, but this is not always a practical solution.

the middle: it can generate rows of $C^{-1}\mathbf{Z}$ in an online manner, but it requires $O(b \cdot d)$ space, where b is the number of bands in the matrix C, a hyper-parameter chosen to minimize expected error. Algorithm 1 and Example B.1 shows how this is done in practice.

2.2 Strategy Optimization

To deploy amplified DP-BANDMF effectively, we must carefully select the matrix \mathbf{C} to minimize the error it introduces during training. The matrix \mathbf{C} and it's number of bands is chosen by solving a numerical optimization problem to minimize the expected total squared error added to the (clipped + aggregated) minibatch gradients during training.

Proposition 2.1 (Expected Error [27, 5]). The expected total squared error of DP-BANDMF given a b-banded strategy matrix C is equal to:

$$\mathbb{E}[\|\mathbf{A}\mathbf{C}^{-1}\mathbf{Z}\|_F^2] = \sigma_{BandMF}^2(\epsilon, \delta, b, k, n)\|\mathbf{C}\|_{1,2}^2\|\mathbf{A}\mathbf{C}^{-1}\|_F^2$$

where $\|\mathbf{C}\|_{1,2}$ is the maximum L_2 column norm of \mathbf{C} and is related to it's sensitivity, and \mathbf{A} is the workload, typically taken to be the lower triangular matrix of ones[20, 9, 6], and $\sigma_{BandMF}(\epsilon, \delta, b, k, n) = \sigma_{SGD}(\epsilon, \delta, bk, n/b)$ is the noise multiplier required to run DP-BANDMF under the given privacy budget.

The optimization problem at the heart of DP-BandMF follows immediately from this expression and is stated below. Note that smaller values of b give better privacy amplification (smaller σ_{BandMF}), but reduces the benefits of correlated noise (more restricted space of strategies). Since b is a discrete parameter, we solve the un-amplified version of the problem for fixed $b \subseteq [1,n]$ (not accounting for σ_{BandMF}), and choose the strategy and number of bands that minimizes expected error accounting for σ_{BandMF} in a brute force manner.

Problem 2.1. Given a workload matrix **A**, and the desired number of bands b, the optimization problem underlying DP-BANDMF can be formulated as:

minimize
$$\|\mathbf{C}\|_{1,2}^2 \|\mathbf{A}\mathbf{C}^{-1}\|_F^2$$
 subject to $\mathbf{C}_{ij} = 0$ if $(j > i)$ or $(i \le j + b)$ (1)

Absent the bandedness constraint, this optimization problem has received considerable attention [27, 42, 31, 9], and the algorithm for solving it in the banded case is closely related [5]. Prior work [5] solves Problem 2.1 by reformulating it in terms of the object $\mathbf{X} = \mathbf{C}^{\mathsf{T}}\mathbf{C}$. This reformulation is convex and unconstrained, meaning standard optimization tools like L-BFGS can efficiently find the best solution with access to an oracle that computes the loss and gradient with respect to \mathbf{X} , while the problem as it is stated in Problem 2.1 is *not* convex with respect to \mathbf{C} [27, 42, 31, 30]. The drawback of this solution approach is that it materializes several $n \times n$ matrices in each iteration, even though there are only roughly $b \cdot n$ free (non-zero) variables. As a result, it requires $O(n^3)$ time and $O(n^2)$ space to evaluate the objective once, and cannot be practically done beyond $n \approx 10^4$.

3 Approach

In this section, we propose two approaches to *implicitly* compute the objective function, bypassing the need to materialize $n \times n$ matrices explicitly. These innovations enable scalability up to and beyond $n = 10^5$ and $n = 10^6$ respectively, opening up new application domains for DP-BANDMF. For simplicity, we specialize the presentation to the Prefix workload, banded strategies, the expected total squared error objective (Proposition 2.1). In App. C, we show that the same core approach taken here easily translates to more general classes of workloads, strategies, and objective functions.

3.1 Efficient strategy optimization

The complexity of solving Problem 2.1 using L-BFGS is proportional to the complexity of evaluating the objective function and it's corresponding gradient. Our first key idea to scale up DP-BANDMF is to utilize Algorithm 1 to efficiently evaluate the objective function. Specifically, we will materialize one row of \mathbf{AC}^{-1} at a time and compute the norm in an online fashion by utilizing Algorithm 1.

Let Θ be a $b \times n$ matrix of parameters which will define our banded strategy matrix $\mathbf{C}(\Theta)$. We define $\mathbf{C}(\Theta)$ to be the column-normalized b-banded matrix satisfying: $C_{ij} = \Theta_{(j-i+1)j}/\sqrt{\sum_{i=1}^b \Theta_{ii}^2}$. By

Algorithm 2 (Efficient) Expected Total Squared Error

```
Input: \Theta \in \mathbb{R}^{b \times n}

Output: \|\mathbf{AC}(\Theta)^{-1}\|_F^2

\mathbf{b}_0 = \mathbf{0}

\mathbf{loss} = 0

for i = 1, \dots, n do

c_i = \sqrt{\sum_{j=1}^b \Theta_{ji}^2}

\mathbf{y}_i = (\mathbf{e}_i - \sum_{j=1}^b \Theta_{ji} \mathbf{y}_j)/\Theta_{1i}

\mathbf{b}_i = \mathbf{b}_{i-1} + \mathbf{y}_i \cdot c_i

\mathbf{loss} + \mathbf{e}_i^{\mathsf{T}} \mathbf{b}_i

return \mathbf{loss}
```

construction, we have $\|\mathbf{C}(\Theta)\|_{1,2} = 1$. Thus, to evaluate the objective function we simply need to compute $\|\mathbf{AC}(\Theta)\|_F^2$, and Algorithm 2 gives an algorithm for doing that efficiently.

Each iteration of Algorithm 2 requires $O(n \cdot b)$ time, as the vectors \mathbf{e}_i and \mathbf{y}_i are size n, and there is a sum over b such vectors. Thus, the total time complexity of Algorithm 2 is $O(n^2 \cdot b)$. The algorithm must keep track of $\mathbf{y}_{i-b}, \ldots, \mathbf{y}_i$ in each iteration, and hence the space complexity is $O(n \cdot b)$. This is a factor $\frac{n}{b}$ improvement in both the time and space complexity of DP-BANDMF, which can be substantial when the number of bands is small (which we will demonstrate in Section 4). While Algorithm 2 is specialized to the class of (column-normalized) banded strategies and the Prefix workload, the core approach is easy to generalize to other parameterized classes of strategies and more general workloads, as we discuss in App. C.

Our L-BFGS algorithm also requires the gradient of the objective function to run efficiently. We do not derive that here, but rather rely on Jax's reverse-mode auto-differentiation capabilities instead [3]. Depending on how the gradients are computed, the gradient computation can be more time and memory intensive than the loss calculation. We provide some experiments on the scalability of this approach in Section 4. Using these ideas, we can scale DP-BANDMF up to roughly $n \approx 10^5$ under reasonable time and memory constraints, without sacrificing any solution quality over prior work [5].

3.2 Optimizing Banded Toeplitz Strategies

In this section, we explore another technique that is even more scalable, while only sacrificing a small amount in terms of expected error. Our key idea is to restrict attention to the special class of *banded Toeplitz strategies*. By exploiting the special structure of this class of strategies, we can evaluate the objective function using only $O(n \cdot b)$ time and O(n) space, and scale strategy optimization up to and beyond $n \approx 10^6$, as we show below:

Proposition 3.1 (Banded Toeplitz Expected Total Squared Error). Let $\theta \in \mathbb{R}^b$ be Toeplitz coefficients, such that $\mathbf{C}(\theta)_{ij} = \theta_{i-j+1}$, and let $\mathbf{w} = \mathbf{C}(\theta)^{-1}\mathbf{1}$. The expected total squared error is equal to:

$$\|\mathbf{C}(\boldsymbol{\theta})\|_{1,2} = \|\boldsymbol{\theta}\|_2 \qquad \|\mathbf{A}\mathbf{C}(\boldsymbol{\theta})^{-1}\|_F^2 = \sum_{i=1}^n (n-i+1)w_i^2$$

Proof. Note that both **A** and $C(\theta)$ are lower triangular Toeplitz matrices, which have a number of nice properties [15, 23, 10]. If $C(\theta)$ is invertible, then its inverse is also a lower triangular Toeplitz matrix. Moreover, multiplication is commutative within this class, and therefore $AC^{-1}(\theta) = C^{-1}(\theta)A$, and this product is itself a lower triangular Toeplitz matrix. As such, it is completely defined by its first column **w**, which we can obtain by multiplying $C^{-1}(\theta)$ by the first column of **A**, which is **1**. The squared Frobenius norm can be calculated directly over this vector by observing that w_i appears (n - i + 1) times.

The complexity of evaluating the objective function is determined by the cost of solving the linear Toeplitz system $\mathbf{w} = \mathbf{C}(\boldsymbol{\theta})^{-1}\mathbf{1}$, which can be done with Algorithm 1 in $O(n \cdot b)$ time and O(b) space. We note that this approach generalizes to any Toeplitz-structured workload, as we show in App. C.

Column Normalization In general the column norms of Toeplitz matrices are not all equal, a property that optimal strategies are known to have [43, 42, 30] and a property built-in to DP-BANDMF [5]. When the number of bands is small, the loss in solution quality due to not column normalizing is generally small, as we demonstrate in Section 4. Moreover, we can always normalize the columns of the banded Toeplitz matrices as a post-processing step after strategy optimization, which we recommend in practice.

3.3 Distributed Noise Generation

The overhead incurred by DP-BANDMF at training-time depends on the specific application, training configuration, and *implementation*. While prior implementations of DP-MF-style algorithms have added noise on a single machine [20, 8, 6], we note that Algorithm 1 can be translated to an embarrassingly parallel algorithm since each coordinate of the noise vectors are treated identically. In particular, each machine is in charge of producing a different slice of the noise vectors \mathbf{y}_i . This insight allows DP-BANDMF to run on larger models and more bands than was previously possible.

To better understand the scalability limits of DP-BANDMF, it is useful to look at a few illustrative examples. Relevant factors that influence scalability include: the number of bands, the number of (trainable) model parameters, the complexity of the forward/backward pass, and the number of machines being trained on. We focus primarily on memory consumed by DP-BANDMF, as our experience suggests that is often the limiting factor. When the computations fit in memory, the overhead of noise generation is generally small compared to gradient computation, especially when using virtual batches which is common in DP training. The examples below demonstrate that we can run DP-BANDMF with a modest to large number of bands under reasonable compute budgets.

Example 3.1. Suppose we want to train a 4 million parameter model on a single GPU with a memory limit of 1 GB. We can afford to store roughly 64 copies of the model assuming each parameter is represented as a 4-byte float. This allows us to use roughly 64 bands overall.

Example 3.2. Now suppose we want to train a larger 128 million parameter model in parallel on 64 machines, which is useful/needed to get the large batch sizes usually used with large models and DP training. By parallelizing the noise generation code across these 64 machines, we can afford to store 2 copies of the model per machine, allowing us to use roughly 128 bands overall.

Example 3.3. Now suppose we want to finetune an 8 billion parameter model on 64 machines, and use a parameter-efficient fine-tuning method such as LoRA [19, 41]. Further, assume the number of learnable finetuning parameters is 4 million. Now, the cost of the forward/backward pass completely dwarfs any overhead of noise generation. We can store 64 copies of the model per machine, and parallelize computation across 64 machines, allowing us to run DP-BANDMF with up to 4096 bands.

4 Empirical Results

In this section, we empirically evaluate our proposed strategy optimization algorithms in terms of solution quality and scalability. Then, we conduct experiments and perform analysis to understand the optimal number of bands as a function of the relevant parameters. Our analysis reveals that in many scenarios of practical interest the optimal number of bands is small, and consequently the overhead of DP-BANDMF at training time is acceptably small. Our experiments focus on RMSE, which we compute in closed form using Proposition 2.1, dividing by n and taking the square root.

4.1 Solution Quality

We begin by evaluating the solution quality of three strategies: (1) the banded Toeplitz strategy described in Section 3.2, (2) the column-normalized version of the above, and (3) the implicitly optimized banded strategy described in Section 3.1. We compare the expected mean squared error of these strategies with the one produced by the explicit optimization method from DP-BANDMF [5].

We optimize strategies for $n=1,2,4,\ldots,2^{20}$ and $b=1,2,4,\ldots,1024$. Strategy optimization is done on an NVIDIA V100 Tensor Core GPU for a maximum of 10,000 iterations. We use strategy (2) above to initialize our optimization of strategy (3), which improves stability and convergence speed. We show results for two slices in Figures 2a and 2b, one where n=1024 and b is varied, and one where b=16 and n is varied. The findings and trends were similar for other choices of n and b. The highlights from this experiment are three-fold:

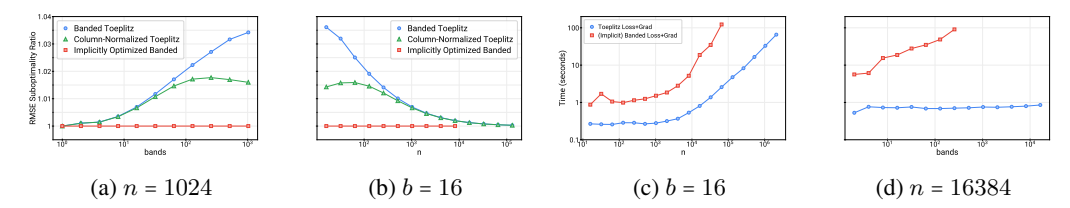


Figure 2: (a-b) Ratio of RMSE of each strategy to the optimal banded strategy from DP-BANDMF as a function of b and a. (c-d) Per-iteration runtime of our two strategy optimization approaches as a function of a and a.

- Our implicit strategy optimization algorithm for banded matrices converges to the same solution as prior work [5] for all n and b tested (where the latter successfully ran). This is encouraging in light of the fact that we directly optimize C (rather than X = C^TC [5]) and Problem 2.1 is not convex with respect to C.
- 2. The optimal Toeplitz strategy matrix is 0-4% suboptimal, with suboptimality increasing with the number of bands and decreasing with the number of iterations. For large n and small b, which is the regime of most interest, the suboptimality is less than 1%, indicating full banded optimization may not provide much benefit.
- 3. The column-normalized optimal Toeplitz matrix always has better RMSE than the non-column-normalized version, with suboptimality ranging from 0-2%. Column normalization has little effect when b is small relative to n. This is not surprising, as all but the last b columns already have equal norms in a banded Toeplitz matrix.

4.2 Scalability

Next, we evaluate the scalability of our strategy optimization algorithms by measuring the wallclock time required to evaluate the loss and gradient. In Figure 2c we vary n for fixed b=16, and in Figure 2d we vary b for fixed n=16384. Figure 2c reveals we can scale up to n=65536 and b=16 with a per-iteration runtime of around 100 seconds for our banded strategy optimizer. Our Toeplitz optimizer is far more scalable, requiring only a few seconds for n=65536 and scaling up to n=2,097,152 in the same amount of time. While 100 seconds per iteration is a nontrivial amount of time, the optimizations generally converge quickly, and 10 or 100 iterations is likely sufficient to realize most of the benefit. Moreover, strategy optimization is an up-front cost that can be done offline before model training starts in most applications. Finally, since we generally need to add more noise as n increases, it seems unlikely that training for so many steps would be helpful in practice.

4.3 Optimal Number of Bands

We will now explore the RMSE of DP-BANDMF as a function of the number of bands and discuss intuitions for selecting it in practice. The recommendation given by the original DP-BANDMF work [5] was to simply try a bunch of values for b, and choose the best one by computing the expected error using Proposition 2.1. In this section, we provide a more fundamental understanding, along with a simple heuristic that can be used to quickly estimate it without writing any code.

Figure 3a plots the RMSE of DP-BANDMF as a function of b for various numbers of epochs at $\epsilon=1$. Results for $\epsilon=8$ are shown in Figure 7 of App. D. The results look similar for other values of ϵ , but required number of epochs to get reasonable RMSE increases, and the best number of bands does increase as well holding all else constant (as will be shown later).

With b=1, DP-BANDMF is equivalent to DP-SGD, and only benefits from amplification (not correlated noise). With $b=\frac{n}{k}$, DP-BANDMF only benefits from correlated noise (not amplification) and closely resembles DENSE-DP-MF. By focusing on the left side of the plot where b=1, we see that the utility of DP-SGD rapidly degrades when the number of epochs falls below 32. However, with only 32 epochs, DP-SGD has nearly the same RMSE as full-batch gradient descent (16384 epochs). By looking at the right side of the plot, where $b=\frac{n}{k}$, we can get a sense of how DENSE-DP-MF behaves. In particular, it achieves worse RMSE than DP-SGD when the number of epochs is large (and utility is the best), but it degrades more gracefully than DP-SGD, offering better utility

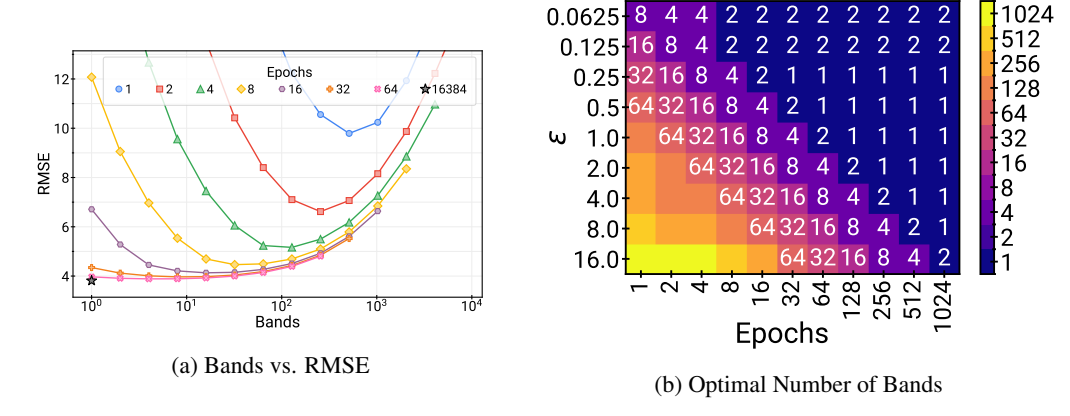


Figure 3: (a) RMSE of DP-BANDMF as a function of b for various epochs, with fixed $(\epsilon, \delta) = (1, 10^{-8})$ and n = 16384. (b) Optimal number of bands (within a factor of 2) for DP-BANDMF as a function of the privacy budget and the number of epochs, fixing n = 4096 and $\delta = 10^{-8}$.

in the small-epoch regime. Finally, by looking at the minimum of each curve, we can understand how DP-BANDMF behaves. It offers the best of both worlds: full-batch DP-SGD-level performance when the number of epochs is sufficiently large, and even more graceful degradation of RMSE with respect to number of epochs than DENSE-DP-MF. Specifically, with only two epochs, DP-BANDMF has less than double the RMSE of full-batch DP-SGD.

Figure 3b shows the optimal number of bands for various numbers of epochs and various values of ϵ , fixing n=4096 and $\delta=10^{-8}$ (results look largely similar for other values of n). This plot has some interesting structure: first, the optimal number of bands decreases with epochs and increases with ϵ in a fairly predictable way. Specifically, the dependence appears roughly linear in in both parameters: doubling ϵ leads to double the optimal number of bands, while doubling the number of epochs leads to half the optimal number of bands. A good rule of thumb: if $\hat{k} \approx \epsilon \sqrt{n}$ is the (minimum) number of epochs where b=1 is optimal, then to run for $k<\hat{k}$ epochs we should roughly set $b=\hat{k}/k$.

4.4 Amplification vs Noise Correlation

In Figure 4, we measure the benefit of privacy amplification and noise correlation respectively, by comparing the RMSE of DP-BANDMF with DENSE-DP-MF and DP-SGD. Figure 4a shows that amplification is most beneficial when both ϵ and epochs are small. However, even up to $\epsilon = 8$, there is a meaningful improvement in RMSE of $\approx 15\%$. Figure 4b shows that correlated noise is most beneficial when ϵ is large and epochs is small, and lines up very nicely with Figure 3b. In the most extreme setting, the RMSE of DP-BANDMF can be $9\times$ lower than DP-SGD. With larger epochs or smaller ϵ , the benefit of correlated noise decreases, confirming it is most useful in compute-constrained settings. It is interesting to note that when the number of epochs is large (but still well less than n), Amplified DP-SGD and Unamplified DP-BANDMF both achieve similar RMSE, despite being very different mechanisms. Moreover, the RMSE in these settings nearly matches the RMSE attained by full-batch DP-SGD, even with many fewer epochs (512 instead of 16384).

4.5 RMSE vs. Learning Performance

Thus far we have primarily focused on RMSE, but this is just a proxy for what we really care about: training-time learning performance. In Figure 5 we aim to understand the relationship between RMSE and learning performance across a range of DP-MF strategies. Our goal is not to compare different mechanisms across a different privacy budgets, as this has been done in prior work [5, 4, 9].

For each strategy under consideration, we train a BertTiny model with per-example clipping and correlated noise addition with a range of noise multiplies spanning 2-3 orders of magnitude. We tune the learning rate for each setting and report results for the best value found. If RMSE was a good

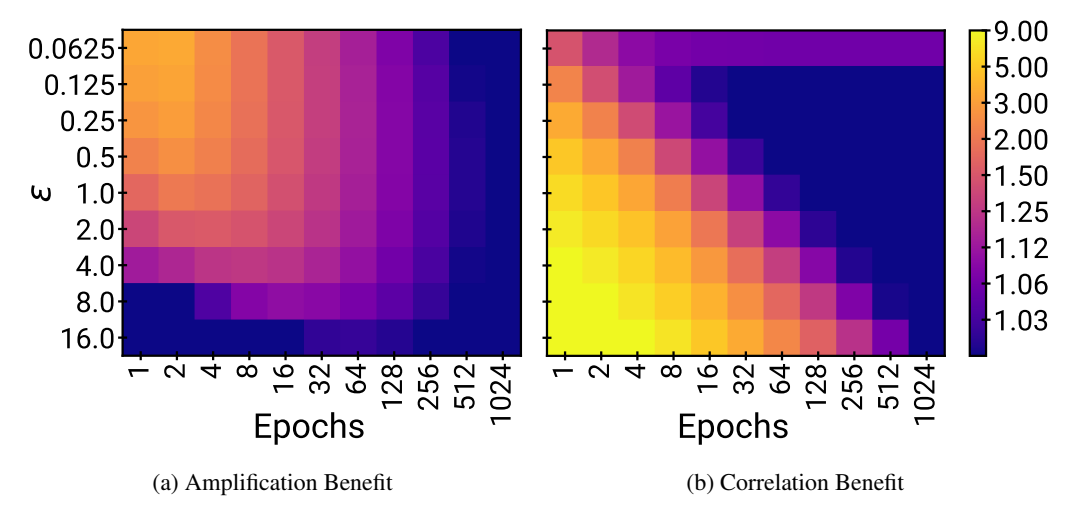


Figure 4: (a) Ratio of RMSE between Unamplified DP-BANDMF (b = n/k) and DP-BANDMF, which measures the benefit of amplification in different settings. (b) Ratio of RMSE between Amplified DP-SGD (b = 1) and DP-BANDMF, which measures the benefit of correlated noise in different settings. Both plots show results for n = 16384.

predictor, we would expect the RMSE vs. cross entropy lines for different strategies to approximately line up.

Figure 5a shows that for an adaptive optimizer and the same RMSE, strategies with fewer bands provide better learning performance. Extrapolating these results, in order for DENSE-DP-MF to outperform DP-SGD in learning performance, it would have to have significantly lower RMSE. Figure 5b shows that for a non-adaptive optimizer, the lines for 1-, 8-, and 64-banded strategies all line up, indicating that RMSE is a reasonable predictor of learning performance. However, there is still a gap between 512-banded DP-BANDMF and BLT-DP-MF (5000 bands), where fewer bands achieves better learning performance for the same RMSE. Overall, the RMSE is lower with the adaptive optimizer as well. Figure 8 in App. D shows that max error also appears to be an unreliable proxy for learning performance, and the same observations hold there as well.

Taken together, these results suggest that one should set bands more conservatively than suggested by RMSE alone to optimize learning performance. This has the dual advantage of improving both utility and training-time memory complexity. Designing a new objective function for DP-MF-style mechanisms that targets adaptive optimizers and is predictive across a wide range of strategies remains an important open question.

5 Related Work

More DP-MF Variants Koloskova et al. and Choquette-Choo et al. [21, 4] revisit the objective underlying DP-MF and propose new variants based on their analysis. Like us, Henzinger et al. [16, 17] and Choquette-Choo et al. [4] use Toeplitz strategies, and bypass the $O(n^3)$ runtime of strategy optimization. However, they consider "full" Toeplitz matrices and do not address the $O(n \cdot d)$ training-time memory overhead of the algorithm, preventing scalability in large-scale settings.

Scalable Approaches to the Matrix Mechanism The optimization problem we studied in this work dates back to the Matrix Mechanism [25], and has been the subject of intense research for a different problem domain: answering workloads of linear counting queries over discrete databases [25, 27, 42, 30, 31, 40, 35, 14, 29, 26, 40]. Like us, McKenna et al. and Xiao et al. [31, 40] restrict attention to special classes of strategies that enable efficient strategy optimization. By exploiting the special structure in these strategies, they scale up to and beyond $n \approx 10^9$, but the specific strategies considered in those works do not directly apply in the context of iteratively training ML models.

Concurrently with our work, Dvijotham et al. proposed BLT-DP-MF [32], a memory-efficient approximation of single-epoch DENSE-DP-MF. Their method reduces training-time memory com-

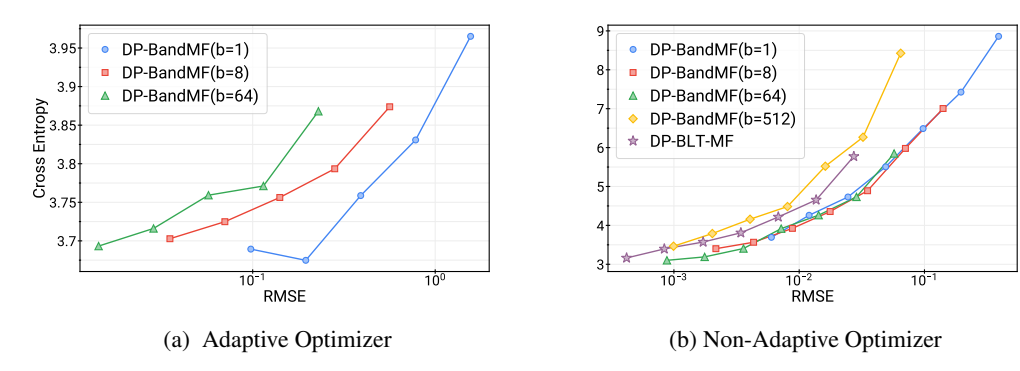


Figure 5: RMSE vs. Learning Performance (evaluation cross entropy) with an adaptive optimizer (a) and a non-adaptive optimizer (b). In both (a) and (b), a 4M parameter BertTiny model is trained on the StackOverflow dataset for various noise multipliers.

plexity to $O(c \cdot d)$ for small and configurable c (e.g., c = 5), with only a minor sacrifice in RMSE compared to DENSE-DP-MF. BLT-DP-MF also enables strategy optimization to scale to an arbitrary number of training iterations. However, our focus is on scaling up multi-epoch DP-BANDMF, while BLT-DP-MF focuses on single-epoch DENSE-DP-MF. Although DP-BANDMF generally outperforms DENSE-DP-MF [5], amplification provides limited benefits in the single-epoch, large ϵ regime. In this setting, DP-BANDMF requires a large number of bands, making BLT-DP-MF a nice alternative.

Empirical work on private ML Many papers have identified using large batches and training for many epochs as a crucial way to improve privacy utility tradeoffs in practice [7, 36, 2, 33, 28, 18, 37]. This is not surprising, and is also supported by our analysis in Section 4.3. Enabling large batch training via efficient per-example gradient clipping algorithms is thus an important research and engineering challenge that has received considerable attention [24, 39, 8, 22].

6 Limitations

Here we discuss two limitations of this paper. First, the number of bands needed to maximize utility may differ from the number of bands that is feasible to use under compute constraints. In Section 4.3 we provided an argument that in the regimes of most practical interest, the number of bands will be small. However, it is conceivable for there to be situations when the optimal number of bands is larger than what can be supported under compute constraints, in which case it would be nice to have an alternative to DP-BANDMF with a configurable memory footprint, independent of the number of bands. Second DP-BANDMF relies on Poisson sampling to form minibatches, which can be tricky to integrate into modern ML infrastructure due to variable batch sizes. Furthermore, privacy amplification is what allows DP-BANDMF to outperform DENSE-DP-MF in RMSE, and why the optimal number of bands is typically small. Without it, DP-BANDMF would need n/k bands and may be infeasible to run for large n and small k.

7 Discussion and Future Work

In this work, we proposed techniques to scale DP-BANDMF to a large number of training rounds needed to support training of large models in multi-machine environments. Our innovations enable scalability beyond $n=10^6$ training iterations, which is likely to be enough for DP training applications where each gradient measurement comes with a privacy cost that must be considered judiciously. Our experiments and analysis on RMSE provide a comprehensive understanding of how DP-BANDMF can be expected to perform in a variety of settings, and our experiments on BERTTINY provide new insights about the relationship between expected error and learning performance. We provide an improved understanding of the performance characteristics of MF-style algorithms, and increased clarity on the relationship between them and DP-SGD. This can be helpful for practitioners to understand if DP-BANDMF is right for their application.

Acknowledgements We would like to thank Keith Rush for discussions about scalable implementations of correlated noise generation plus for sharing knowedge about distributed Jax. We would also like to thank Brendan McMahan and Arun Ganesh for providing comments on a draft of this work.

References

- [1] Martin Abadi, Andy Chu, Ian Goodfellow, H Brendan McMahan, Ilya Mironov, Kunal Talwar, and Li Zhang. Deep learning with differential privacy. In *Proceedings of the 2016 ACM SIGSAC conference on computer and communications security*, pages 308–318, 2016.
- [2] Rohan Anil, Badih Ghazi, Vineet Gupta, Ravi Kumar, and Pasin Manurangsi. Large-scale differentially private bert. In *Findings of the Association for Computational Linguistics: EMNLP* 2022, pages 6481–6491, 2022.
- [3] James Bradbury, Roy Frostig, Peter Hawkins, Matthew James Johnson, Chris Leary, Dougal Maclaurin, George Necula, Adam Paszke, Jake VanderPlas, Skye Wanderman-Milne, and Qiao Zhang. JAX: composable transformations of Python+NumPy programs, 2018.
- [4] Christopher A Choquette-Choo, Krishnamurthy Dj Dvijotham, Krishna Pillutla, Arun Ganesh, Thomas Steinke, and Abhradeep Guha Thakurta. Correlated noise provably beats independent noise for differentially private learning. In *The Twelfth International Conference on Learning Representations*, 2023.
- [5] Christopher A Choquette-Choo, Arun Ganesh, Ryan McKenna, H Brendan McMahan, John Rush, Abhradeep Guha Thakurta, and Zheng Xu. (amplified) banded matrix factorization: A unified approach to private training. Advances in Neural Information Processing Systems, 36, 2024.
- [6] Christopher A Choquette-Choo, Hugh Brendan Mcmahan, J Keith Rush, and Abhradeep Guha Thakurta. Multi-epoch matrix factorization mechanisms for private machine learning. In *International Conference on Machine Learning*, pages 5924–5963. PMLR, 2023.
- [7] Soham De, Leonard Berrada, Jamie Hayes, Samuel L Smith, and Borja Balle. Unlocking high-accuracy differentially private image classification through scale. *arXiv* preprint *arXiv*:2204.13650, 2022.
- [8] Carson Denison, Badih Ghazi, Pritish Kamath, Ravi Kumar, Pasin Manurangsi, Krishna Giri Narra, Amer Sinha, Avinash V Varadarajan, and Chiyuan Zhang. Private ad modeling with dp-sgd. *arXiv preprint arXiv:2211.11896*, 2022.
- [9] Sergey Denisov, H Brendan McMahan, John Rush, Adam Smith, and Abhradeep Guha Thakurta. Improved differential privacy for sgd via optimal private linear operators on adaptive streams. *Advances in Neural Information Processing Systems*, 35:5910–5924, 2022.
- [10] Hamide DOGAN, Kachmar KHALİL, and Luis R SUAREZ. Some results on the ideals of real-valued lower triangular toeplitz matrices. *Turkish Journal of Mathematics and Computer Science*, 9:50–54, 2018.
- [11] Vadym Doroshenko, Badih Ghazi, Pritish Kamath, Ravi Kumar, and Pasin Manurangsi. Connect the dots: Tighter discrete approximations of privacy loss distributions. *Proceedings on Privacy Enhancing Technologies*, 2022.
- [12] Cynthia Dwork. Differential privacy. In *International colloquium on automata, languages, and programming*, pages 1–12. Springer, 2006.
- [13] Cynthia Dwork. Differential privacy: A survey of results. In *International conference on theory and applications of models of computation*, pages 1–19. Springer, 2008.
- [14] Alexander Edmonds, Aleksandar Nikolov, and Jonathan Ullman. The power of factorization mechanisms in local and central differential privacy. In *Proceedings of the 52nd Annual ACM SIGACT Symposium on Theory of Computing*, pages 425–438, 2020.
- [15] Gene H Golub and Charles F Van Loan. Matrix computations. JHU press, 2013. See Section 4.7.
- [16] Monika Henzinger and Jalaj Upadhyay. Constant matters: Fine-grained complexity of differentially private continual observation using completely bounded norms. Cryptology ePrint Archive, 2022.

- [17] Monika Henzinger, Jalaj Upadhyay, and Sarvagya Upadhyay. Almost tight error bounds on differentially private continual counting. In *Proceedings of the 2023 Annual ACM-SIAM Symposium on Discrete Algorithms (SODA)*, pages 5003–5039. SIAM, 2023.
- [18] Shlomo Hoory, Amir Feder, Avichai Tendler, Sofia Erell, Alon Peled-Cohen, Itay Laish, Hootan Nakhost, Uri Stemmer, Ayelet Benjamini, Avinatan Hassidim, et al. Learning and evaluating a differentially private pre-trained language model. In *Findings of the Association for Computational Linguistics: EMNLP 2021*, pages 1178–1189, 2021.
- [19] Edward J Hu, Phillip Wallis, Zeyuan Allen-Zhu, Yuanzhi Li, Shean Wang, Lu Wang, Weizhu Chen, et al. Lora: Low-rank adaptation of large language models. In *International Conference* on Learning Representations, 2021.
- [20] Peter Kairouz, Brendan McMahan, Shuang Song, Om Thakkar, Abhradeep Thakurta, and Zheng Xu. Practical and private (deep) learning without sampling or shuffling. In *International Conference on Machine Learning*, pages 5213–5225. PMLR, 2021.
- [21] Anastasiia Koloskova, Ryan McKenna, Zachary Charles, John Rush, and H Brendan McMahan. Gradient descent with linearly correlated noise: Theory and applications to differential privacy. *Advances in Neural Information Processing Systems*, 36, 2024.
- [22] Weiwei Kong and Andres Munoz Medina. A unified fast gradient clipping framework for dp-sgd. *Advances in Neural Information Processing Systems*, 36, 2024.
- [23] Dan Kucerovsky, Zikun Wang, and Neville Robbins. On some properties of toeplitz matrices. *Cogent Mathematics*, 3(1):1154705, 2016.
- [24] Jaewoo Lee and Daniel Kifer. Scaling up differentially private deep learning with fast per-example gradient clipping. *Proceedings on Privacy Enhancing Technologies*, 2021(1), 2021.
- [25] Chao Li, Michael Hay, Vibhor Rastogi, Gerome Miklau, and Andrew McGregor. Optimizing linear counting queries under differential privacy. In *Proceedings of the twenty-ninth ACM SIGMOD-SIGACT-SIGART symposium on Principles of database systems*, pages 123–134, 2010.
- [26] Chao Li and Gerome Miklau. Optimal error of query sets under the differentially-private matrix mechanism. In *Proceedings of the 16th International Conference on Database Theory*, pages 272–283, 2013.
- [27] Chao Li, Gerome Miklau, Michael Hay, Andrew McGregor, and Vibhor Rastogi. The matrix mechanism: optimizing linear counting queries under differential privacy. *The VLDB journal*, 24:757–781, 2015.
- [28] Xuechen Li, Florian Tramer, Percy Liang, and Tatsunori Hashimoto. Large language models can be strong differentially private learners. In *International Conference on Learning Representations*, 2021.
- [29] Ryan McKenna, Raj Kumar Maity, Arya Mazumdar, and Gerome Miklau. A workload-adaptive mechanism for linear queries under local differential privacy. *Proceedings of the VLDB Endowment*, 13(11), 2020.
- [30] Ryan McKenna, Gerome Miklau, Michael Hay, and Ashwin Machanavajjhala. Optimizing error of high-dimensional statistical queries under differential privacy. *Proceedings of the VLDB Endowment*, 11(10), 2018.
- [31] Ryan McKenna, Gerome Miklau, Michael Hay, and Ashwin Machanavajjhala. Optimizing error of high-dimensional statistical queries under differential privacy. *Journal of Privacy and Confidentiality*, 13(1), 2023.
- [32] H Brendan McMahan, Krishna Pillutla, Thomas Steinke, Abhradeep Thakurta, et al. Efficient and near-optimal noise generation for streaming differential privacy. *arXiv preprint* arXiv:2404.16706, 2024.
- [33] H Brendan McMahan, Daniel Ramage, Kunal Talwar, and Li Zhang. Learning differentially private recurrent language models. In *International Conference on Learning Representations*, 2018.
- [34] Ilya Mironov. Rényi differential privacy. In 2017 IEEE 30th computer security foundations symposium (CSF), pages 263–275. IEEE, 2017.

Symbol	Domain	Meaning				
\overline{n}	\mathbb{N}_{+}	number of training iterations				
d	\mathbb{N}_{+}	model dimensionality				
k	\mathbb{N}_{+}	number of epochs				
q	(0,1]	minibatch sampling probability				
$ar{b}$	N ₊	number of bands				
σ	\mathbb{R}_{+}	noise multiplier				
\mathbf{A}	$\mathbb{R}^{n \times n}$	lower triangular ones matrix				
${f Z}$	$\mathbb{R}^{n \times d}$	Gaussian noise, $Z_{ij} \sim \mathcal{N}(0, \sigma^2)$				
\mathbf{C}	$\mathbb{R}^{n \times n}$	DP-BANDMF strategy matrix				
$\mathbf{C}(oldsymbol{ heta})$	$\mathbb{R}^{n \times n}$	Parameterized strategy matrix				
\mathbf{e}_i	\mathbb{R}^n	<i>i</i> th indicator vector				
$\ \cdot\ _{1,2}$	\mathbb{R}_{+}	maximum L_2 column norm				
$\sigma_{SGD}(\epsilon,\delta,q,n)$	\mathbb{R}_{+}	DP-SGD noise multiplier				
	111 1 70	11 CAT (C				

- Table 1: Table of Notation
- [35] Aleksandar Nikolov, Kunal Talwar, and Li Zhang. The geometry of differential privacy: the sparse and approximate cases. In *Proceedings of the forty-fifth annual ACM symposium on Theory of computing*, pages 351–360, 2013.
- [36] Natalia Ponomareva, Hussein Hazimeh, Alex Kurakin, Zheng Xu, Carson Denison, H Brendan McMahan, Sergei Vassilvitskii, Steve Chien, and Abhradeep Guha Thakurta. How to dp-fy ml: A practical guide to machine learning with differential privacy. *Journal of Artificial Intelligence Research*, 77:1113–1201, 2023.
- [37] Ossi Räisä, Joonas Jälkö, and Antti Honkela. Subsampling is not magic: Why large batch sizes work for differentially private stochastic optimisation. arXiv preprint arXiv:2402.03990, 2024.
- [38] David Sommer, Sebastian Meiser, and Esfandiar Mohammadi. Privacy loss classes: The central limit theorem in differential privacy. *Cryptology ePrint Archive*, 2018.
- [39] Pranav Subramani, Nicholas Vadivelu, and Gautam Kamath. Enabling fast differentially private sgd via just-in-time compilation and vectorization. *Advances in Neural Information Processing Systems*, 34:26409–26421, 2021.
- [40] Yingtai Xiao, Guanlin He, Danfeng Zhang, and Daniel Kifer. An optimal and scalable matrix mechanism for noisy marginals under convex loss functions. *Advances in Neural Information Processing Systems*, 36, 2024.
- [41] Da Yu, Saurabh Naik, Arturs Backurs, Sivakanth Gopi, Huseyin A Inan, Gautam Kamath, Janardhan Kulkarni, Yin Tat Lee, Andre Manoel, Lukas Wutschitz, et al. Differentially private fine-tuning of language models. In *International Conference on Learning Representations*, 2021.
- [42] Ganzhao Yuan, Yin Yang, Zhenjie Zhang, and Zhifeng Hao. Convex optimization for linear query processing under approximate differential privacy. In *Proceedings of the 22nd ACM SIGKDD International Conference on Knowledge Discovery and Data Mining*, pages 2005–2014, 2016.
- [43] Dan Zhang, Ryan McKenna, Ios Kotsogiannis, Michael Hay, Ashwin Machanavajjhala, and Gerome Miklau. Ektelo: A framework for defining differentially-private computations. In Proceedings of the 2018 International Conference on Management of Data, pages 115–130, 2018.

A Notation

B DP-BANDMF Example

C Generalizations to Other Strategy and Workload Classes

Our presentation in Section 3.1 focused on the Prefix workload and the class of (column-normalized) banded matrices and Toeplitz matrices. However, our core approach also applies to a broader set of strategies in workloads, as we show in this section.

Example B.1 (DP-BANDMF). The matrix below is the optimal 3-banded strategy matrix C configured for 9 training iterations. (Informal 4) DP-BANDMF with minibatch sampling probability of $q \le 1/3$ enjoys the same privacy guarantees as 3 iterations of DP-SGD with sampling probability 3q. The vectors $\mathbf{y}_1, \dots, \mathbf{y}_9$ are added to the minibatch gradients during training, and can be computed efficiently in an online fashion with $O(b \cdot d)$ space using Algorithm I, exemplified below:

0.740	0	0	0	0	0	0	0	0 1	$^{-1}$ [\mathbf{z}_1]	- [:	\mathbf{y}_1	
0.500	0.822	0	0	0	0	0	0	0	$ \mathbf{z}_2 $		\mathbf{y}_2	
0.450	0.492	0.876	0	0	0	0	0	0	\mathbf{z}_3		\mathbf{y}_3	
0	0.286	0.395	0.821	0	0	0	0	0	$ \mathbf{z}_4 $		\mathbf{y}_4	
0	0	0.278	0.462	0.855	0	0	0	0	\mathbf{z}_5	= :	\mathbf{y}_5	
0	0	0	0.335	0.442	0.882	0	0	0	\mathbf{z}_6		\mathbf{y}_6	
0	0	0	0	0.272	0.403	0.892	0	0	$ \mathbf{z}_7 $		\mathbf{y}_7	
0	0	0	0	0	0.243	0.409	0.936	0	$ \mathbf{z}_8 $	1 1	\mathbf{y}_8	
0	0	0	0	0	0	0.194	0.353	1.000	$[\mathbf{z}_9]$		\mathbf{y}_9	

```
• \mathbf{y}_1 = \mathbf{z}_1 / 0.740
```

•
$$\mathbf{y}_2 = (\mathbf{z}_2 - 0.500 \mathbf{y}_1) / 0.822$$

•
$$\mathbf{y}_3 = (\mathbf{z}_3 - 0.492\mathbf{y}_2 - 0.450\mathbf{y}_1)/0.876$$

```
• \mathbf{y}_4 = (\mathbf{z}_4 - 0.395\mathbf{y}_3 - 0.286\mathbf{y}_2)/0.821
```

• . . .

•
$$\mathbf{y}_9 = (\mathbf{z}_9 - 0.353\mathbf{y}_8 - 0.194\mathbf{y}_7)/1.000$$

Algorithm 3 Streaming Linear Operator for Prefix

```
Input: stream of vectors \mathbf{z}_1, \dots, \mathbf{z}_n \in \mathbb{R}^d, where \mathbf{Z} is the matrix with rows \mathbf{z}_i.
```

Output: Y = AZ, one row at a time.

 $\begin{aligned} & \textbf{for } i = 1, \dots, n \ \textbf{do} \\ & \mathbf{y}_i = \mathbf{y}_{i-1} + \mathbf{z}_i \\ & \textbf{yield } \mathbf{y}_i \end{aligned}$

Figure 6: Algorithm for streaming matrix multiplication by a Prefix matrix. To simplify the presentation, we use the convention that out-of-bounds indexing into a matrix or vector returns 0.

C.1 Streaming Linear Operators

We begin by providing a definition for a Streaming Linear Operator:

Definition C.1 (Streaming Linear Operator (SLO)). A Streaming Linear Operator is a function that consumes a sequence of vectors $\mathbf{z}_1, \dots, \mathbf{z}_n$ as input one at a time, and produces a sequence of vectors $\mathbf{y}_1, \dots, \mathbf{y}_n$ one at a time such that \mathbf{y}_i is a linear function of $\mathbf{z}_1, \dots, \mathbf{z}_i$. We say a SLO is b-buffered if it only requires storing a state of size at most b vectors.

We note that there is a one-to-one correspondence between SLOs and lower triangular matrices. The Prefix matrix can be represented as a 1-buffer SLO, shown in Figure 6. Banded lower triangular matrices and their inverses can be represented as b-buffer SLOs, as shown in Algorithm 1. The heavyball momentum + learning rate cooldown workload studied in prior work [8, 6] can also be represented as a 2-buffer SLO.

C.2 Efficiently Optimizing Parameterized Strategies via SLOs

Recall that computing the objective function efficiently is the core requirement for performing efficient strategy optimization over the space of strategies. As long as we can express this function in terms of Jax primitives, we can rely on auto-differentiation tools to compute the gradients and perform the optimization. Hence, our focus in this section is on generalizing generalize Algorithm 2 to handle *any* workload represented as a SLO, and *any* parameterized strategy whose inverse is a SLO, and *any* differentiable aggregator of the per-query expected squared errors.

Algorithm 4 is an algorithm to calculate the per-query expected error of any workload and parameterized strategy represented as a pair of SLOs. The time and memory complexity of this algorithm

Algorithm 4 Efficiently Evaluating the Per Query Error

```
Input: SLO for C(\Theta)^{-1}, SLO for A

Output: \mathbf{b}_i^{\mathsf{T}} \mathbf{b}_i, one entry at a time, where \mathbf{B} = \mathbf{AC}(\Theta)^{-1}

\mathbf{b}_0 = \mathbf{0}

for i = 1, ..., n do

\mathbf{y}_i = SLO_{C^{-1}}(\mathbf{e}_i)

\mathbf{b}_i = SLO_A(\mathbf{y}_i)

yield \mathbf{b}_i^{\mathsf{T}} \mathbf{b}_i
```

depends only on the complexity of the underlying SLO implementations. In general, for a b_1 -buffer SLO for ${\bf C}^{-1}$ and b_2 -buffer SLO for ${\bf A}$, the time and memory complexity of Algorithm 4 is $O(n^2(b_1+b_2))$ and $O(n(b_1+b_2))$ respectively. We note that the per-query-error can be combined with any (sub)-differentiable aggregator to get a scalar-valued loss function that can be optimized. In this paper, our focus was on expected total squared error, which is simply a sum of the per-query squared errors. However, the max expected error is another natural choice that has been sometimes used in prior work [32, 16]. The "best" loss function to use, i.e., the one that best correlates with learning performance, is still an open question.

C.3 Efficiently Optimizing Banded Toeplitz Strategies for Toeplitz Workloads

In this section, we show that we can efficiently calculate the expected per-query squared error for a banded Toeplitz strategy on *any* Toeplitz workload with a minor modification to Proposition 3.1. These generalizations do not affect the time or memory complexity of the algorithm.

Proposition C.1 (Banded Toeplitz Expected Per-Query Squared Error). Let λ , $\theta \in \mathbb{R}^b$ be Toeplitz coefficients for \mathbf{A} and \mathbf{C} respectively. The expected square error (excluding sensitivity) on the i^{th} query can be evaluated as $\sum_{j=1}^{i} w_j^2$ where $\mathbf{w} = \mathbf{C}(\theta)^{-1} \lambda$

D Experiments

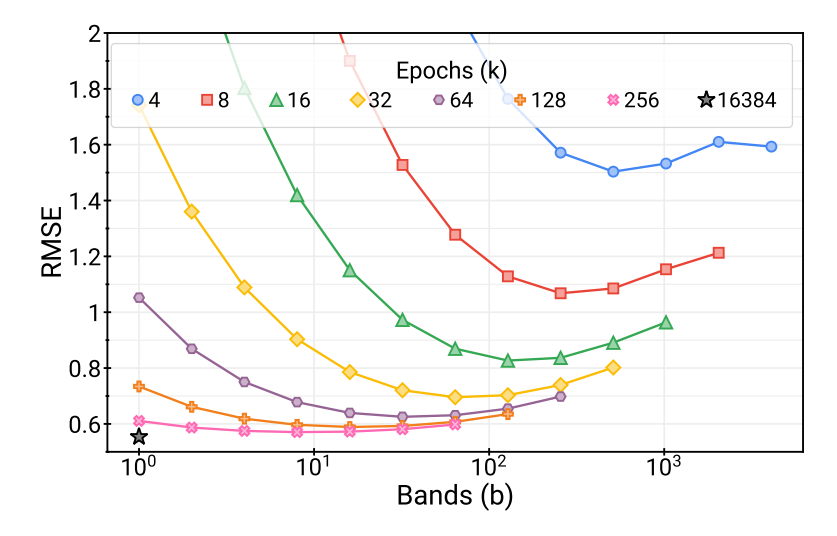


Figure 7: RMSE of DP-BANDMF as a function of b for various epochs, with fixed $(\epsilon, \delta) = (8, 10^{-8})$ and n = 16384. With b = 1, DP-BANDMF is equivalent to DP-SGD, and only benefits from amplication (not correlated noise). With $b = \frac{n}{k}$, DP-BANDMF only benefits from correlated noise (not amplification) and closely resembles DENSE-DP-MF. The best RMSE is obtained somewhere in the middle, with the both the best RMSE and corresponding value of b decreasing with epochs. By using DP-BANDMF instead of DP-SGD, one can run for far fewer epochs without sacrificing nearly as much utility.

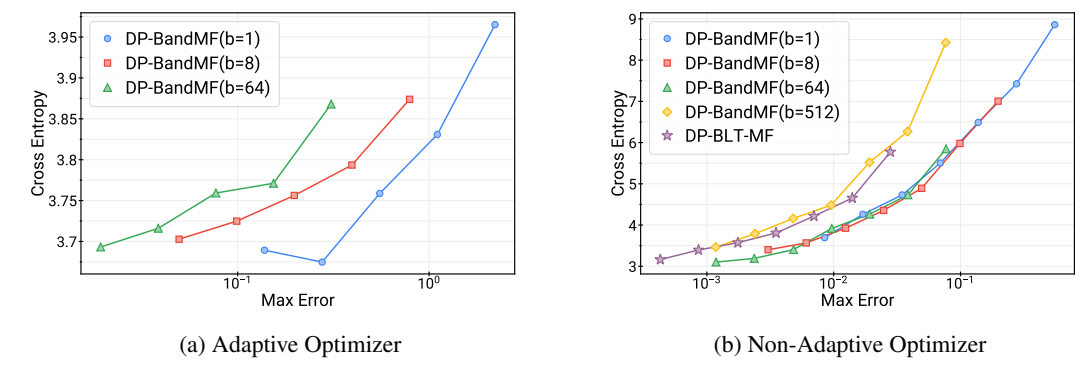


Figure 8: Max Per-Query Error vs. Learning Performance (evaluation cross entropy) with an adaptive optimizer (a) and a non-adaptive optimizer (b). In both (a) and (b), a 4M parameter BertTiny model is trained on the StackOverflow dataset for various noise multipliers.